Talanta 112 (2013) 95–100

Contents lists available at SciVerse ScienceDirect

Talanta

journal homepage: www.elsevier.com/locate/talanta

A gravity-induced flow injection system for surface plasmon resonance biosensor

Chao Zhou, Ying Mu*, Mengchao Yang, Qi Song, Ying Zhang, Zhongyu Wu, Liancheng Xiang, Wei Jin, Qinhan Jin*

Research Center for Analytical Instrumentation, Institute of Cyber-Systems and Control, State Key Laboratory of Industrial Control Technology, Zhejiang University, Hangzhou, China

ARTICLE INFO

Article history:
Received 31 December 2012
Received in revised form
10 March 2013
Accepted 14 March 2013
Available online 26 March 2013

Keywords:
Power-free
Surface plasmon resonance
Gravity-induced
Flow injection analysis

ABSTRACT

A number of portable surface plasmon resonance (SPR) devices have been developed for point-of-care (POC) testing. Meanwhile, micropumps have been fabricated to be integrated into these devices for flow injection analysis (FIA). However, the (micro) pumps, the tubes and their external control units were space-consuming. Here we developed a power-free flow injection analysis (FIA) method for SPR detection based on a gravity-induced flow injection (gFI) system. The gFI system was tubeless and did not need to be controlled. The fluid was driven into the detection areas by its own gravitational force. A transition channel was used to increase the liquid-level difference between the inlet reservoir and the outlet reservoir. After a liquid sample was placed in the inlet reservoir, the flow rate of the liquid sample was increased in the transition channel. Before it arrived at the sensing surface, the flow rate of the sample was steady (with an error of less than 10%). The fluctuation of the flow rate had an influence on the SPR response signal, which was successfully denoised using an internal reference. With the gFI system, the SPR imaging biosensor was able to perform real-time detection manually. The SPR responses of DNA hybridization and protein immobilization were successfully obtained.

1. Introduction

Surface plasmon resonance (SPR) biosensors have shown great potentials in a wide range of areas, from genetic analysis [1] to high-throughput detection of the proteins [2] to living cell identification [3]. A tendency of its development was the miniaturization of the SPR devices for point of care (POC) testing, from Spreeta 2000 [4] to portable SPR devices [5–8] to palm-sized SPR or SPR imaging (SPRi) devices [9–13]. Many applications for POC testing have been reported [14]. However, these developments were generally focused on the miniaturization of the internal optical structures. Most of the SPR devices needed commercially available peristaltic or syringe pumps [15]. To further minimize the system size and the biosample volume, some micro flow injection systems were developed. For example, a micro flow injection system was powered by the traveling wave that was induced by the piezoelectric actuator array. The system was much smaller than the conventional flow injection systems, but it still needed some space-consuming parts, e.g.: the tubes or the electronic control unit.

Recently, power-free flow injection systems have attracted many attentions. These systems could provide controllable analysis with minimal system size, reagent consumption and so on. A number of power sources were used to drive the fluid in the power-free systems, including: the degassed polydimethylsiloxane (PDMS) [16], gravitational forces of the fluid [17], surface tension of the fluid [18], capillarity forces of the channel [19], on-chip chemical reactions [20], and so on. Though most of these methods could be used to perform the flow injection analysis (FIA), many of them were not suitable to maintain a steady flow and a large sample volume. The flow rate and the sample volume were essential to obtain the real-time kinetic information of the biomolecule interaction, because the binding rate between the ligand and the analyte was proportional to the cubic root of the flow rate under mass transport limitation [21,22]. Thus the power-free flow injection methods were studied in terms of the flow rate, the sample volume and the manipulation procedure. Degassed PDMS pumps, for example, were used to restore vacuum power that propelled the sample into the microchip. Limited by its size, the sample volume was limited to tens of microliter. The value was much smaller than the amount needed for the surface based biosensor to reach the equilibrium binding state. On the other side, the sample volumes of the gravity-induced systems were commonly more than hundreds of microliter, which was enough for a typical SPR binding [22–24]. As reported, in the gravity-induced flow injection system, the flow rate was increasingly steady when the liquid-level difference was increased [25].

The gFI system was suitable for SPR biosensor; however, previous designs were not suitable for practical application. First,

* Corresponding authors. Tel.: +86 571 88208383; fax: +86 571 88208382.
E-mail addresses: muying@zju.edu.cn (Y. Mu), qhjin@zju.edu.cn (Q. Jin).

0039-9140/$ - see front matter © 2013 Elsevier B.V. All rights reserved.
http://dx.doi.org/10.1016/j.talanta.2013.03.037

some of the gFI systems required extra parts, e.g: a moving platform [26]. Second, the integrated gFI systems were tilted to increase the liquid-level difference [17]. The liquid-level difference was limited by the distance between the inlet and outlet of the gFI system. Third, the waste was usually guided to a very large reservoir or manually removed [27]. The waste surface should be well controlled automatically. To realize the power-free flow injection analysis for SPR biosensor, we have recently developed a gravity-induced flow injection (gFI) system. The gFI system comprised of a transition channel between the inlet reservoir and the sensing microchannels, as shown in Fig. 1. The liquid-level difference was increased by the transition channel. The speed of the newly added liquid was increased in the transition channel. Thus, when the liquid arrived at the sensing surface, its velocity had already reached a steady value. The waste fluid was removed by a multiple layers of tissue paper that was place on the top of the outlet. The influence of the flow rate fluctuation was eliminated by using an internal reference (the reference area shared the same microchannel with the detection area [28]). Real time SPR responses of DNA hybridization and protein immobilization were obtained successfully. The results demonstrated that the gFI system was capable of flow injection analysis for SPR detection. To the best knowledge of the authors, the gFI system was the first power-free flow injection system designed for SPR detection.

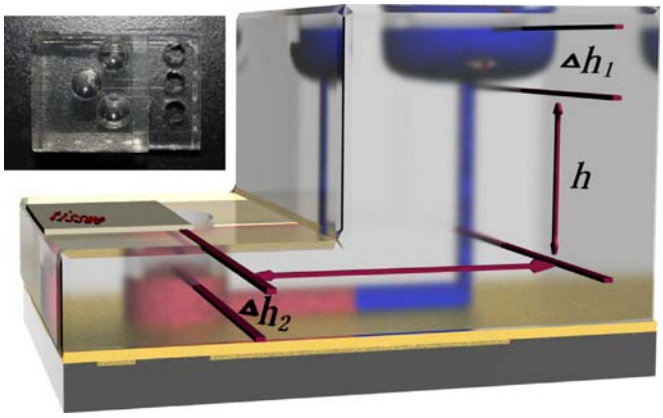

Fig. 1. The 3-D structure diagram of the gFI system. The liquid-level difference between the inlet reservoir (with blue liquid) and the outlet reservoir (with red liquid) was determined by the transition channel. The gravitational forces continuously pushed the newly added biosample (blue) into the microchannel, and the waste (red) was removed by the tissue paper placed on the top of the outlet reservoir. The inlet photograph was the top view of the gFI system which contained three parallel flow injection units. The size of the gFI system was about 40 mm long, 30 mm wide, 25 mm high. (For interpretation of the references to color in this figure legend, the reader is referred to the web version of this article.)

2. Experimental part

2.1. Fabrication and operation of the gFI system

The glass mold of the microchannels (100 μm deep, 500 μm wide, 20 mm long) was fabricated by standard soft lithography and wet etching as describe elsewhere [29]. The inlet reservoir, the outlet reservoir and the transition channel were fabricated using a home-made metallic mold. As shown in Fig. 1, the inlet reservoir (6 mm diameter, 4 mm high) was connected to the microchannels via the transition channel (0.7 mm diameter, 12.5 mm or 25.5 mm long), and the outlet reservoir (4 mm diameter, 5 mm high) was connected to the microchannels directly. The gFI system was made of PDMS (ratio 10: 1) with a baking time of 2 h.

The gFI system was adhered to the gold surface and was operated in the way that was illustrated in Scheme 1. First, the gFI system was filled with buffer, which spontaneously flew to the outlet reservoir. The buffer was retained by the capillary force at the inlet opening of the transition channel. Then the following liquid sample (or buffer) was placed in the inlet reservoir and flew through the sensing surface. The process was repeated until all the samples were injected sequentially, as shown in Video. 1. All the liquid samples were added by using a pipette manually. The waste was removed by a multiple layers of tissue paper (3 mm long, 2 mm wide, and 16 layers). A single layer of tissue paper was able to remove 50 μL waste, thus more than 800 μL waste could be removed automatically. The evaporation rate of the absorbed waste was tested to be more than 4 μL/min at a relative humidity of 30% and temperature of 20 °C. If the average flow rate of the biosample liquid was 10 μL/min, the tissue paper could continuously work for 2 h.

Supplementary material related to this article can be found online at http://dx.doi.org/10.1016/j.talanta.2013.03.037.

2.2. SPR device

The SPR device employed the typical Kretschmann structure. The incident angle of the LED light beam was fixed at the angle of 72°. The collimated LED beam passed through the p-polarizer, the BK7 prism, the 10 nm filter (630–640 nm), and finally arrived at the CMOS detector. A BK7 slide (30 mm long, 20 mm wide) was mounted on the bottom side of the prism using the refractive index matching liquid. The gold film that was deposited on the

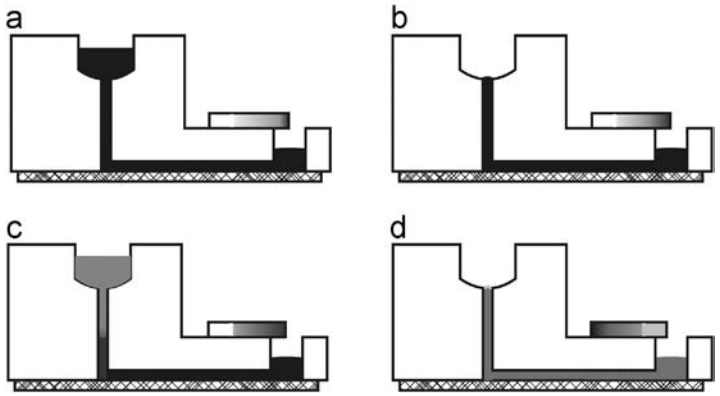

Scheme 1. The workflow of the gFI system. a, The gFI system was pre-filled with PBS buffer; b, The buffer flew to the outlet spontaneously and stopped by the inlet capillary force of the transition channel; c, New sample was added and flew towards the sensing surface; d, The new sample flew to the outlet and stopped at the end of the transition channel.

slide had a thickness of 45 nm. Finally, the gFI system was adhered to the gold surface.

2.3. Reagents

All oligonucleotides were synthesized and then purified by high performance liquid chromatography by Sangon (Shanghai, China). Reagent grade chemicals were also purchased from Sangon. The sequences of synthesized single strand DNAs (ssDNAs) were 5′–SH-$(CH_2)_6$-TCCCGTTGGTGGGATG-3′ (SH-DNA) and 5′-$(CH_2)_6$-CATCCCACCAACGGGA-3′ (CP-DNA) respectively. The buffer for DNA hybridization was PBS (0.01 M phosphate, 1 M NaCl, pH 7.4). The tissue paper was purchased from X & Y (Shenzhen, China).

2.4. Detection of the DNA hybridization

The detection procedure was shown in Scheme 2. One side of the gold film surface was modified with glutathione (10 mg/mL) for 1 h, while the other side was left empty. The modified area was used as the reference. When the sample of thiol-terminated single strand DNA flew through the gold surface, the SH-DNA did not immobilize on the glutathione modified area. Approximately 100 μL thiolated ssDNA (2 μM) was used. The surface was rinsed with 100 μL PBS buffer, followed by 80 μL complementary DNA (2 μM) and excessive PBS buffer.

3. Results and discussion

3.1. The flow rate of the liquid within the gFI system

The hydrodynamic resistance of the gFI system comprised of the resistances of the microchannel, the transition channel and the reservoirs. As the resistances in the reservoirs and the transition channel were much smaller than that in the microchannel, they were neglected for simplicity [27]. In the microfluidic systems with laminar flow, the volumetric flow rate is governed by Hagen-Poiseuille equation. For a rectangular channel with a high width-to-height ratio, the equation could be written as:

$$Q = \Delta P x y^3 / 12\, L\mu \quad (1)$$

where Q is the volumetric flow rate, L is the length of the microchannel, μ is the water viscosity, and x and y are the width and height of the microchannel. As reported earlier, the hydrostatic pressure difference ΔP at the microchannel was possibly proportional to the liquid-level difference H between the inlet fluid and outlet fluid [17]. The pressure is given by Pascal's law:

$$\Delta P = \rho g H \quad (2)$$

where the ρ is the density of the fluid and g is the gravity acceleration. Accordingly, the volumetric flow rate was possibly proportional to liquid-level difference H. However, the liquid-level difference H was changing during the injection process. As shown in Fig. 1, during the injection process, the inlet liquid-level was decreased by Δh_1 and the outlet liquid-level might increase by Δh_2. In the designed gFI system, Δh_1 was about 3.5 mm corresponding to 100 μL fluid, and the maximum of Δh_2 was measured to be smaller than 3 mm. As seen in Video. 2, the surface of the outlet liquid reached the multiple layers of tissue paper and was quickly absorbed by the tissue paper, before a protruding liquid surface was formed.

Supplementary material related to this article can be found online at http://dx.doi.org/10.1016/j.talanta.2013.03.037.

To determine the flow rate, the lateral image of the inlet reservoir was captured every 2 s. The number of changed pixels was calculated and converted to the flow rate. By this means, the calculated flow rate was plotted in Fig. 2. Two gFI systems with different transition channels were compared. To obtain a good comparison between the gFI systems, the sample volume was 200 μL for the 25.5 mm transition channel and 100 μL for the 12.5 mm transition channel. From the result, the gFI system with the longer transition channel showed a better performance

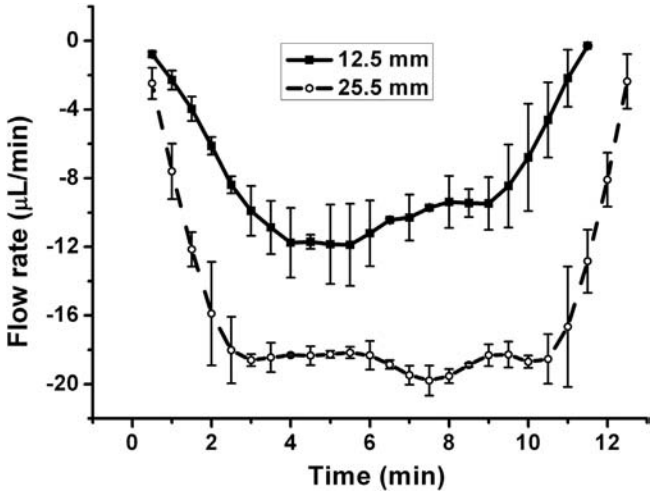

Fig. 2. The volumetric flow rate was obtained by calculating the captured lateral images of the inlet reservoir. 100 μL or 200 μL PBS buffer was visualized by the blue dyes. The volume of the sample was calculated every 2 s.

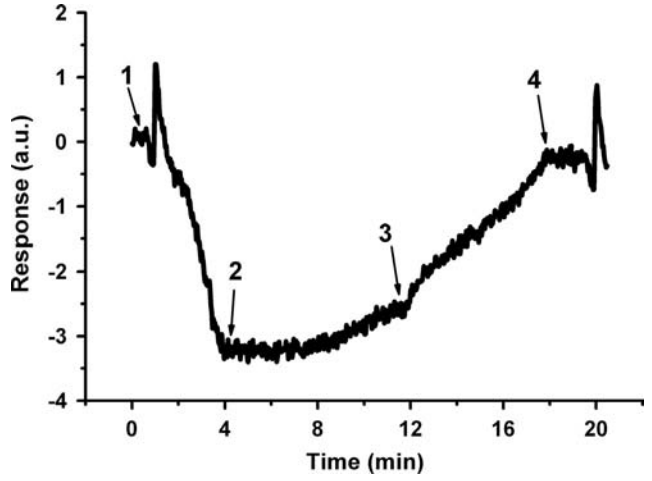

Fig. 3. The SPR response of the PBS buffer. When the PBS was added, a sharp fluctuation was observed (point 1). Then the flow rate of the buffer reached a stable level (point 2). At the end of the flow injection (point 3), the SPR response of the buffer returned to the original level (point 4).

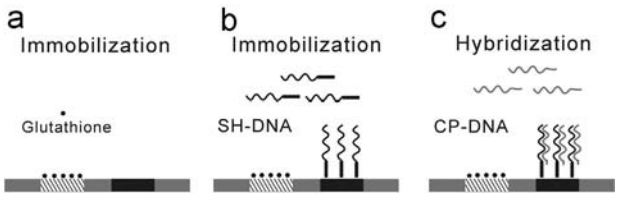

Scheme 2. The process of the kinetic study of the DNA hybridization using the internal reference. a, The gold surface of the biosensor was partially blocked by using high concentration of glutathione (blue areas). b, The SH-DNA (black) flew through the sensing surface and immobilized on the unmodified gold surface. c, The CP-DNA (grey) was hybridized with the immobilized SH-DNA.

in terms of acceleration time and flow rate stability. As shown by the solid line in Fig. 2, the sampling procedure could be divided into three stages: the accelerated stage (from 0 min to 3 min), the relatively stable stage (from 3 min to 9 min) and the decelerated stage (from 9 min to 13 min). The accelerated and decelerated stages were short and unstable. As discussed later, their influences were limited and could be neglected. In the relatively stable stage, the error of the flow rate was less than 10% (from 10 μL/min to 12 μL/min). As the binding rate between the ligand and the analyte was proportional to the cubic root of the flow rate under mass transport limitations, the expected kinetic information might have an error of less than 5%. A tendency of decrease in the flow rate was observed, probably due to the descent of the inlet liquid-level. The fluctuation of the flow rate was possibly due to the fluctuation of the outlet liquid-level. Clearly, as the length of the transition channel *h* was increased, the relative standard deviations of the flow rate would be smaller in the second stage.

3.2. Influence of the flow rate

As influenced by the sudden change in the flow rate, the SPR response was observed to have the same tendency of changes. As shown in Fig. 3, the SPR response of the PBS buffer was divided into three parts. Before the fluid was placed in the inlet, the fluid within the gFI system was static. When the fluid was placed (point 1), a quick and sharp fluctuation in SPR response was monitored. The flow rate of the fluid was increased to a relatively steady value. The corresponding SPR response of the PBS was dramatically decreased within 4 min (from point 1 to point 2). Then, from point 2 to point 3, the SPR response reached a steady value and decreased slightly. At point 3, a sudden increase in SPR response indicated the nearing completion of the flow injection. Different from the monitored flow rate, SPR response did not return to its original position immediately. It took 5 min to reach an equilibrium state (point 4). It was noticed that the SPR response was changed at point 4 compared to that at point 1. The change

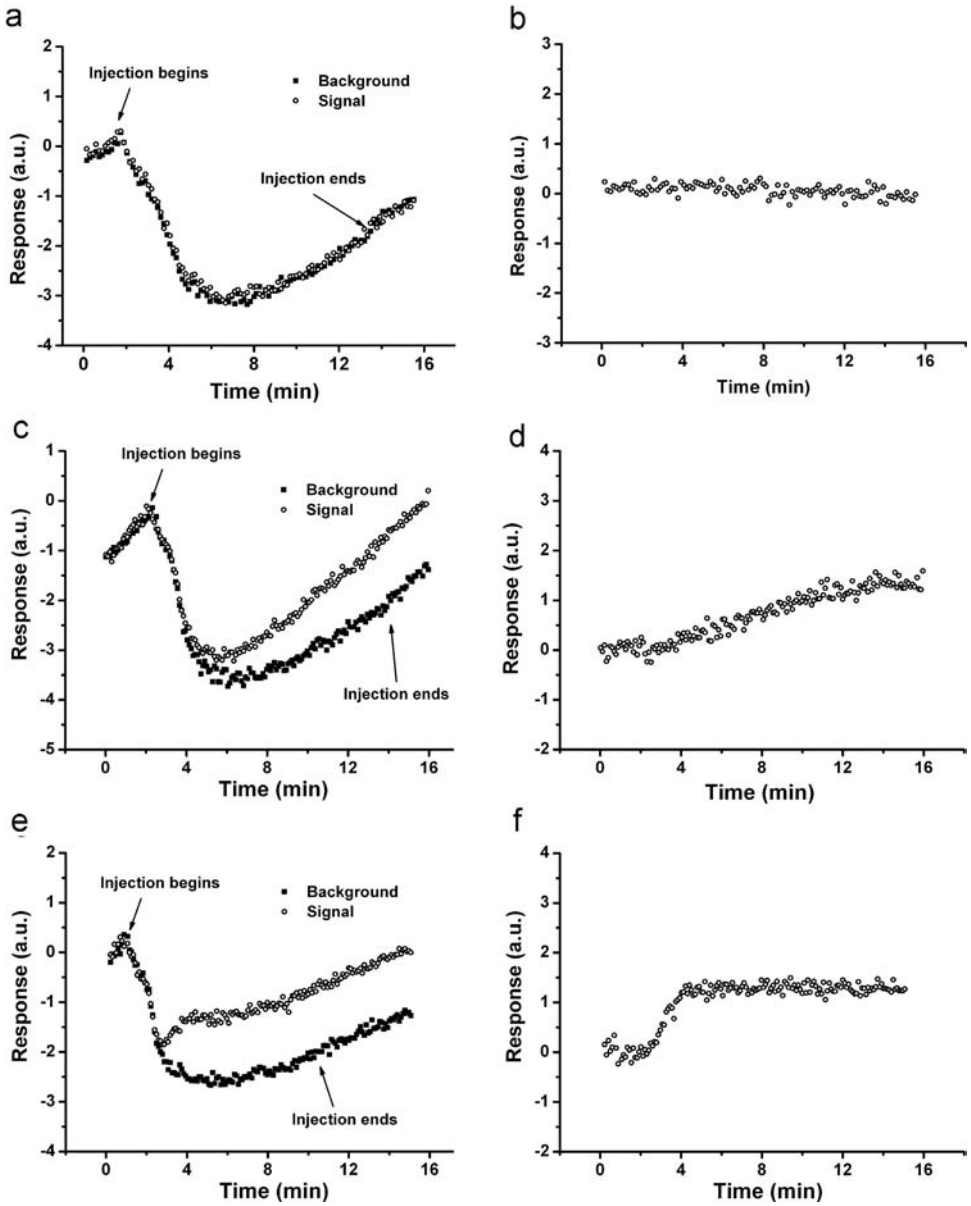

Fig. 4. The SPR response of the ssDNA hybridization. Both the signal and the background were recorded. The subtracted responses were shown aside. a and b were the responses of the PBS buffer; c and d were the responses of the SH-DNA immobilization; e and f were the responses of the DNA hybridization.

Table 1
The summary of DNA hybridization on surface.

	Low probe density	High probe density
Probe density [33]	$< 3 \times 10^{12}$ probes/cm^2	$> 5 \times 10^{12}$ probes/cm^2
Analysis mode [34–36]	Langmuir adsorption model	(Diffusion-limited) Langmuir adsorption model
Association rate [34,37–39]	$1.8–11.0 \times 10^4$ M^{-1} s^{-1}	$< 5.7 \times 10^4$ M^{-1} s^{-1}
Hybridization efficiency [33]	$> 75\%$	$< 50\%$

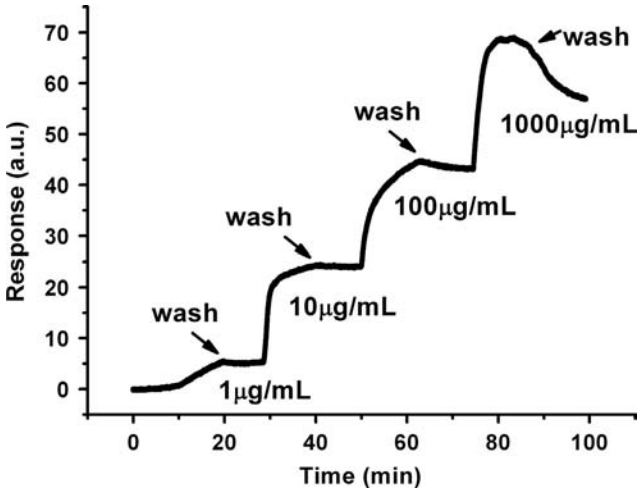

Fig. 5. The immobilization of BSA was performed sequentially. The varying concentrations of BSA were 1 μg/mL, 10 μg/mL, 100 μg/mL and 1000 μg/mL.

was possibly caused by the flow rate fluctuation. Obviously, the fluctuation of the SPR response could be termed as the system noise and would decrease the sensitivity of the biosensor. Elimination of the noise was essential to detect small signals, and thus the internal reference was used.

3.3. Detection of small signals

The internal reference was determined to be a sensing area that shared the same microchannel and biosample with the detection area [28]. Many SPR imaging method used the internal reference that enabled real time compensation for dark current and intensity of the light [30,31]. Moreover, using the internal reference was possible to detect the binding under different buffer condition [28]. Here, the internal reference was used to subtract the noise caused by the flow rate fluctuation. As described in Scheme 2, part of the gold surface was modified with the high concentration glutathione, and thus was insensitive to the binding of other molecules. Then, the SH-DNA and CP-DNA were injected into the sensing area sequentially. As shown in Fig. 4a and b, the SPR response of the signal and background were both generated by the PBS buffer. The subtracted response was flat with the deviation of ± 0.13, which was 10 times smaller than the original SPR response fluctuation. When the thiol-terminated ssDNA immobilized on the unmodified surface, the responses of the signal and background were separated several minutes after the injection began, as shown in Fig. 4c. The subtracted response in Fig. 4d demonstrated that the immobilization occurred about 3 min after the injection began. As shown in Fig. 4e and f, the hybridization with the complementary ssDNA also occurred 3 min after the injection began. Thus the accelerated stage was skipped and had little influence on the association results. As shown in Fig. 4f, the hybridization process was completed within 2 min, and the SPR response was not affected by the flow rate fluctuation in the decelerated stage. In conclusion, provided with enough sample volumes, the binding information was always obtained under a relatively steady flow rate in the gFI system.

The reported results of DNA hybridization on surface were shown in Table 1. Here the ssDNA probes were only immobilized on the gold surface for ten minutes, the probe density should be low according to literatures [32]. Thus the subtracted data of Fig. 4d and f were analyzed with first-order Langmuir equation:

$$\theta = \theta_{max}(1-\exp(-k_{eff}Ct)) \quad (3)$$

where θ is the surface coverage, k_{eff} is the effective association rate for surface hybridization, C is the concentration of the target and t is the time. The association rate of the DNA hybridization was 2.18×10^4 M^{-1} s^{-1}. On the other side, the hybridization efficiency should be high. The conclusion was proven by the SPR response shifts of the probe and target.

3.4. Detection of several injections

As a FIA system, sequential injections of different samples were helpful in understanding the sampling and recovery performance of the gFI system. Here, varying concentrations of bovine serum albumin (BSA) was used. The concentrations were 1 μg/mL, 10 μg/mL, 100 μg/mL and 1000 μg/mL in deionized water respectively. 100 μL of each sample was injected by the gFI system, followed by 100 μL deionized water. The result was shown in Fig. 5. As reported by others, the SPR response of the immobilized protein showed a linear increase in response with the log increase in the applied protein concentration [28].

4. Conclusion

In this paper, a power-free flow injection system for SPR devices was presented. The gFI system was tested to have the ability for FIA with extremely simple operations. From the obtained results, the biomolecule interactions always happened at a steady flow rate. And the biosample volume was adjustable for different purposes. Thus the gFI system was capable of flow injection analysis for the SPR detection. The miniature and power-free flow injection system would open the possibility to build a much more miniature system for point of care testing.

Acknowledgment

The research was supported by the National Natural Science Foundation of China (31070772, 31270907), Doctoral Program of Higher Education of China (20090101110136), Science and Technology Programs of Zhejiang Province, China (2011C37029) and State Key Laboratory of Industrial Control Technology of China.

References

[1] Y. Zhang, Y. Mu, C. Zhou, Q. Song, W. Jin, Q. Jin, Microchim. Acta 177 (2012) 435–441.
[2] X. Yu, X. Ding, F. Liu, Y. Deng, Sensor. Actuat. B-Chem. 130 (2008) 52–58.

[3] V. Chabot, Y. Miron, M. Grandbois, P.G. Charette, Sensor. Actuat. B-Chem. 174 (2012) 94–101.
[4] T.M. Chinowsky, J.G. Quinn, D.U. Bartholomew, R. Kaiser, J.L. Elkind, Sensor. Actuat. B-Chem. 91 (2003) 266–274.
[5] A.N. Naimushin, S.D. Soelberg, D.U. Bartholomew, J.L. Elkind, C.E. Furlong, Sensor. Actuat. B-Chem. 96 (2003) 253–260.
[6] R. Kurita, Y. Yokota, Y. Sato, F. Mizutani, O. Niwa, Anal. Chem. 78 (2006) 5525–5531.
[7] R.J. Whelan, T. Wohland, L. Neumann, B. Huang, B.K. Kobilka, R.N. Zare, Anal. Chem. 74 (2002) 4570–4576.
[8] J.P. Golden, C.R. Taitt, L.C. Shriver-Lake, Y.S. Shubin, F.S. Ligler, Talanta 65 (2005) 1078–1085.
[9] Y. Shin, H.M. Kim, Y. Jung, B.H. Chung, Sensor. Actuat. B-Chem. 150 (2010) 1–6.
[10] H. Šípová, M. Piliarik, M. Vala, K. Chadt, P. Adam, M. Bocková, K. Hegnerová, J. Homola, Procedia Eng. 25 (2011) 148–151.
[11] B.N. Feltis, B.A. Sexton, F.L. Glenn, M.J. Best, M. Wilkins, T.J. Davis, Biosens. Bioelectron. 23 (2008) 1131–1136.
[12] P. Neuzil, J. Reboud, Anal. Chem. 80 (2008) 6100–6103.
[13] H. Nakajima, Y. Harada, Y. Asano, T. Nakagama, K. Uchiyama, T. Imato, N. Soh, A. Hemmi, Talanta 70 (2006) 419–425.
[14] M. Duman, E. Piskin, Biosens. Bioelectron. 26 (2010) 908–912.
[15] T. Suzuki, Y. Teramura, H. Hata, K. Inokuma, I. Kanno, H. Iwata, H. Kotera, Microsyst. Technol. 13 (2007) 1391–1396.
[16] Q. Zhu, Y. Gao, B. Yu, H. Ren, L. Qiu, S. Han, W. Jin, Q. Jin, Y. Mu, Lab. Chip 12 (2012) 4755–4763.
[17] P. Morier, C. Vollet, P.E. Michel, F. Reymond, J.S. Rossier, Electrophoresis 25 (2004) 3761–3768.
[18] G.M. Walker, D.J. Beebe, Lab Chip 2 (2002) 131–134.
[19] N.S. Lynn, D.S. Dandy, Lab. Chip 9 (2009) 3422–3429.
[20] L. Qin, O. Vermesh, Q. Shi, J.R. Heath, Lab. Chip 9 (2009) 2016–2020.
[21] P. Schuck, H. Zhao, Method. Mol. Biol. 627 (2010) 15–54.
[22] J. Bishop, S. Blair, A. Chagovetz, Biosens. Bioelectron. 22 (2007) 2192–2198.
[23] E.T. Krishnamoorthy, A. Carlen, van den Berg, R.B.M. Schasfoort, Sensor. Actuat. B-Chem. 148 (2010) 511–521.
[24] W. Jin, X. Lin, S. Lv, Y. Zhang, Q. Jin, Y. Mu, Biosens. Bioelectron. 5 (2009) 1266–1269.
[25] Z. Cai, H. Chen, B. Chen, C. Huang, Talanta 3 (2006) 895–901.
[26] Y. Guan, Z. Xu, J. Dai, Z. Fang, Talanta 4 (2006) 1384–1389.
[27] I. Chen, E. Lindner, Anal. Chem. 81 (2009) 9955–9960.
[28] M.A. Eddings, J.W. Eckman, C.A. Arana, G.A. Papalia, J.E. Connolly, B.K. Gale, D.G. Myszka, Anal. Biochem. 2 (2009) 309–313.
[29] Z. Jia, Q. Fang, Z. Fang, Anal. Chem. 76 (2004) 5597–5602.
[30] M. Piliarik, M. Bocková, J. Homola, Biosens. Bioelectron. 4 (2010) 1656–1661.
[31] F. Fernández, K. Hegnerová, M. Piliarik, F. Sanchez-Baeza, J. Homola, M.P. Marco, Biosens. Bioelectron. 4 (2010) 1231–1238.
[32] F. Yu, D. Yao, W. Knoll, Nucleic Acids Res. 9 (2004) e75.
[33] A.W. Peterson, R.J. Heaton, R.M. Georgiadis, Nucleic Acids Res. 24 (2001) 5163–5168.
[34] M.R. Henry, P. Wilkins Stevens, J. Sun, D.M. Kelso, Anal. Biochem. 2 (1999) 204–214.
[35] K.A. Peterlinz, R.M. Georgiadis, T.M. Herne, M.J. Tarlov, J. Am. Chem. Soc. 14 (1997) 3401–3402.
[36] D. Erickson, D. Li, U.J. Krull, Anal. Biochem. 2 (2003) 186–200.
[37] M.F. Hagan, A.K. Chakraborty, J. Chem. Phys. 10 (2004) 4958–4968.
[38] K. Tawa, W. Knoll, Nucleic Acids Res 8 (2004) 2372–2377.
[39] J.B. Fiche, A. Buhot, R. Calemczuk, T. Livache, Biophys. J. 3 (2007) 935–946.